A *Trypanosoma cruzi* PHOSPHATIDYLINOSITOL 3-KINASE (TcVps34) IS INVOLVED IN OSMOREGULATION AND RECEPTOR-MEDIATED ENDOCYTOSIS*

Alejandra C. Schoijet[§,¥], Kildare Miranda[¥,¶], Wendell Girard-Dias[¶], Wanderley de Souza[¶], Mirtha M. Flawiá[§], Héctor N. Torres[§], Roberto Docampo[¥,1], and Guillermo D. Alonso[§,2].

[§]Instituto de Investigaciones en Ingeniería Genética y Biología Molecular, Consejo Nacional de Investigaciones Científicas y Técnicas and Departamento de Fisiología, Biología Molecular y Celular, Facultad de Ciencias Exactas y Naturales, Universidad de Buenos Aires, Vuelta de Obligado 2490 (1428), Buenos Aires, Argentina; [¥]Center for Tropical and Emerging Global Diseases and Department of Cellular Biology, University of Georgia, Athens, GA 30602, USA and [¶]Laboratório de Ultraestrutura Celular Hertha Meyer, Instituto de Biofísica Carlos Chagas Filho, Universidade Federal do Rio de Janeiro, Brazil.

Running title: Phosphatidylinositol 3-kinase in *Trypanosoma cruzi*

Trypanosoma cruzi, the etiological agent of Chagas' disease, has the ability to respond to a variety of environmental changes during its life cycle both in the insect vector and in the vertebrate host. Since regulation of transcription initiation seems to be nonfunctional in this parasite, it is important to investigate other regulatory mechanisms of adaptation. Regulatory mechanisms at the level of signal transduction pathways involving phosphoinositides are good candidates for this purpose. Here we report the identification of the first phosphatidylinositol 3-kinase (PI3K) in *T. cruzi,* with similarity with its yeast counterpart, Vps34p. TcVps34 specifically phosphorylates phosphatidylinositol to produce phosphatidylinositol 3-phosphate, thus confirming that it belongs to class III PI3K family. Overexpression of *TcVps34* resulted in morphological and functional alterations related to vesicular trafficking. While inhibition of TcVps34 with specific PI3K inhibitors, such as wortmannin and LY294,000, resulted in reduced regulatory volume decrease after hyposmotic stress, cells overexpressing this enzyme were resistant to these inhibitors. Furthermore, these cells were able to recover their original volume faster than wild type cells when they were submitted to severe hyposmotic stress. In addition, in *TcVps34*-overexpressing cells the activities of vacuolar-H⁺-ATPase and vacuolar H⁺-pyrophosphatase were altered, suggesting defects in the acidification of intracellular compartments. Furthermore, receptor-mediated endocytosis was partially blocked whereas fluid phase endocytosis was not affected, confirming a function for TcVps34 in membrane trafficking. Taken together, these results strongly support that TcVps34 plays a prominent role in vital processes for *T. cruzi* survival such as osmoregulation, acidification and vesicular trafficking.

Phosphatidylinositol 3-kinase (PI3K) activities have been found in all eukaryotic cell types examined up to date (1,2) and are linked to a diverse set of key cellular functions, including cell growth, proliferation, survival, and intracellular trafficking. PI3Ks belong to a large family of enzymes that has been divided into three functional classes on the basis of their protein domain structure, lipid substrate specificity, and regulatory properties. Class I PI3Ks were the first ones to be identified and are important components of the signaling pathways that regulate eukaryotic cell growth (3,4). These PI3Ks have a 110-kDa catalytic subunit that exhibits a substrate preference for PI 4-phosphate and PI 4,5-bisphosphate (5). Class II PI3Ks are less well known but may also function in the regulation of cell growth (5,6), and, additionally, in clathrin-mediated endocytosis (7,8). These enzymes prefer phosphatidylinositol (PI) as substrate but may also utilize PI 4-phosphate. Finally, Class III family of PI3Ks is related to the yeast vacuolar protein sorting 34, Vps34p, and their homologs from other eukaryotes. Vps34p-like kinases specifically phosphorylate PI to produce phosphatidylinositol 3-phosphate (PI 3-P) and are associated with a Vps15p-like protein kinase (6,9). In addition to protein sorting to the vacuole/lysosome, class III PI3Ks have been implicated in several other

membrane transport events, including endocytosis, vesicle acidification and autophagy (10-14).

The protozoan parasite *Trypanosoma cruzi* is the causative agent of Chagas disease in Latin America and the main cause of cardiac death in endemic areas. Currently over 15 million people are infected and other 28 million people are at risk of infection (15). As *T. cruzi* passes through its digenetic life cycle, it encounters extreme fluctuations in external osmolarity. These osmotic fluctuations occur both within the insect gut (16) and also when the parasite moves through the vertebrate host. Previous studies on the response of *T. cruzi* to hyposmotic stress have shown that both insect and vertebrate stages possess a robust regulatory volume decrease (RVD) mechanism that completely reverses cell swelling (17). This process is accomplished by the efflux of various ions and osmolytes (18) and the release of water by the contractile vacuole complex (19). In addition, it has been found that cyclic AMP levels increase when *T. cruzi* epimastigotes are subjected to hyposmotic stress (20). Recently, we described a membrane-associated cAMP-specific phosphodiesterase, TcrPDEC2, which is inhibited by the same inhibitors that affect the RVD of the parasites after hyposmotic stress (20,21). TcrPDEC2 is characterized by the presence of a FYVE domain, which is a phosphoinositide-binding motif. It is known that phosphoinositides serve as lipid signals required for membrane recruitment of several proteins implicated in the regulation of vesicular transport and intracellular protein sorting (22,23), and control the translocation and activity of proteins that contain phosphoinositide-binding motifs such as the FYVE domain, as well as the pleckstrin homology, PX and ENTH domains (23,24).

Since inhibitors of TcrPDEC2 affect osmoregulation in *T. cruzi,* and TcrPDEC2 possesses a FYVE domain able to bind to PI 3-P, we hypothesized that PI 3-P production might have a role in osmoregulation. However, very little is known about the phosphoinositide signaling in trypanosomatids, and up to now only one trypanosome ortholog of *Vps34*, named *TbVps34*, has been described in *Trypanosoma brucei* (25). However, no functional analysis of this enzyme was performed and it is not known whether that enzyme specifically catalyzes PI 3-P production (25). Here we report the identification and functional characterization of TcVps34, the first class III PI3K reported in *T. cruzi*. This study provides new insights into the physiological importance of the PI3K pathway and describes the role of TcVps34 in vital processes, such as osmoregulation, acidification, and receptor-mediated endocytosis.

EXPERIMENTAL PROCEDURES

Chemicals and Reagents- All radiochemicals used in this work were purchased from Dupont NEN Life Science Products Inc., Boston, MA and restriction endonucleases were from New England Biolabs Inc., Beverly, MA. Bacto-tryptose, yeast nitrogen base and liver infusion were from Difco Laboratories, Detroit, MI. All other reagents were purchased from Sigma Chemical Co., St. Louis, MO.

Cell Cultures and Extracts- *T. cruzi* epimastigote forms (CL Brener strain) were cultured at 28°C for 7 days in LIT medium [5 g.l^{-1} liver infusion, 5 g.l^{-1} bacto-tryptose, 68 mM NaCl, 5.3 mM KCl, 22 mM Na_2PO_4, 0.2% (W/V) glucose, 0.002% (W/V) hemin] supplemented with 10% (V/V) newborn calf serum, 100,000 units.l^{-1} penicillin and 100 mg.l^{-1} streptomycin. Cell viability was assessed by direct microscopic examination.

For *T. cruzi* extracts, 10^8 epimastigotes were harvested by centrifugation at 1,500 xg for 10 min and washed two times with phosphate-buffered saline (PBS). Cell pellets were then resuspended in lysis buffer (50 mM HEPES buffer, pH 7.3, containing 0.01 mg.ml^{-1} leupeptin, 25 U.ml^{-1} aprotinin, 0.5 mM phenylmethylsulfonyl fluoride and 14 mM 2-mercaptoethanol), and lysed by six cycles of freezing in liquid N_2 and thawing at 4°C. The total extracts were further centrifuged for 1 h at 100,000 xg to obtain P100 and S100 fractions.

The *Saccharomyces cerevisiae* strain, SEY6210Δ*vps34*::*TRP1* was a kind gift of Dr. Yoshinori Ohsumi (26). Before transformation, this strain was grown at 30°C in synthetic selected media without TRP (Tryptophan), (0.17% (W/V) yeast nitrogen base without amino acids and ammonium sulphate, 0.5% (W/V) ammonium sulphate and 2% (W/V) glucose, supplemented with the corresponding amino acid mixture. Transformant cells were selected in minimal medium without TRP and URA (Uracil).

Cloning of TcVps34 Gene- The gene sequence corresponding to the *T. brucei TbVps34* PI3K (AC159405) was used to screen *T. cruzi* sequences in the GeneDB database using the WU-Blast2 algorithm. Two oligonucleotides carrying hemi-restriction sites (PI3K-Fw-pENTR-KpnI 5´ GGTACCATGGCCACCAACGAAGGCAACGT 3´ and PI3K-Rv-pENTR-XhoI 5´ CTCGAGTTAGTGCCGTGTTGCCTGCGCT 3´) were designed from the identified sequence (Tc00.1047053511903.160). PCR amplifications were carried out using 600-800 ng of *T. cruzi* genomic DNA, 100 ng of each primer, 2.5 mM MgCl$_2$, 0.2 mM dNTPs and 2 units of *Pfu* Ultra High-Fidelity DNA polymerase (Stratagene, La Jolla, CA). Three PCR products were sequenced and compared with the original sequence found at GeneDB. Taken into account that some discrepancies were detected, we reported the obtained sequence to NCBI databank (EU276115)[4].

Sequence Analysis- The search in a *T. cruzi* genome database (http://www.genedb.org) was performed with Wu-Blast2. Sequence identity was analyzed with the BLASTP (URL http://www.ncbi.nlm.nih.gov/blast/index.html) and Clustal W (URL http://www.ebi.ac.uk/clustalw/). Multiple sequence alignment with default parameters setting was used to generate the alignments. Protein domains were determined using SMART (URL http://smart.embl-heidelberg.de/), and PROSITE (URL http://us.expasy.org/prosite/) software.

Southern, Northern and Western blot Analyses- Genomic DNA was purified as described by Pereira et al. (27). Total cellular RNA was isolated from 10^8 epimastigote cells in the exponential growth phase using TRIzol reagents, as described by the manufacturer (Gibco BRL., Life Technologies, Rockville, MD)

Southern and northern blot analyses were performed as described by Alonso et al (28). The products were revealed with a specific 990-bp *TcVps34* probe obtained by digestion of the 2,724-bp fragment with KpnI and PvuII. All probes were labelled with α[P^{32}]-dCTP using the Prime-a-Gene kit (Promega, Madison, WI) following the manufacturer's instructions.

For western blot analysis, 80 μg of P100 and S100 *T. cruzi* fractions were loaded into 8% (W/V) SDS-polyacrylamide gel electrophoresis as described by Laemmli (29) and electrotransferred to Hybond-C membranes (Amersham Pharmacia Biotech, Piscataway, USA). The transferred membranes were then incubated for 4 h with a 1:2,000 dilution of rabbit anti-6-His (Gene Tex, Inc. San Antonio, USA). Detection was carried out by incubating with a 1:5,000 dilution of a goat anti-rabbit conjugated to peroxidase (KPL Inc., Gaithersburg, MA). The latter was developed with the ECL Plus^{TM} Western Blotting Detection System (NEN Life Science Products Inc., Boston, MA).

Complementation Assay- The coding region of *TcVps34* gene was excised from the pDEST17 *E. coli* expression vector (Invitrogen, Carlsbad, CA) and inserted into the KpnI and XhoI restriction sites in the galactose-inducible yeast expression vector pYES2 (URA3; Invitrogen). The yeast *Vps34*-knockout strain, SEY6210 Δ*vps34::TRP1* was transformed with either the empty vector or the vector carrying the *TcVps34* gene, using the lithium acetate procedure (30). Transformed cells were selected in minimal medium (without TRP and URA) at 30°C. For complementation assays, transformed cells were grown to OD$_{600}$ = 1.8-2 with 20% (W/V) glucose as carbon source and plated in the same selective media supplemented with 20% (W/V) galactose and 10% (W/V) raffinose at different dilutions. Plates were incubated at 37°C for three days.

Expression and Purification of Recombinant TcVps34 in E. coli- Full-length *TcVps34* gene was amplified using the following primers carrying hemi-restriction sites: (PI3K-Fw-pENTR-KpnI 5´ GGTACCATGGCCACCAACGAAGGCAACGT 3´ and PI3K-Rv-pENTR-XhoI 5´ CTCGAGTTAGTGCCGTGTTGCCTGCGCT 3´), cloned into pGEM-T Easy plasmid (Promega, Madison, WI) and subcloned into the gateway pENTR3C vector (Invitrogen).

To express the N-terminal His-tagged TcVps34 in *E. coli*, a recombination reaction was performed to transfer the coding sequence from pENTR3C into the pDEST17 expression vector (Invitrogen). The construct (pDEST17-*TcVps34*) was transformed into *BL21(DE3)pLysS* host (*E. coli B, F$^-$, dem, ompT, hsdS, (rb$^-$, m$_B$$^-$), galλ(DE3), [pLysS, cam^r]*) and the recombinant protein was induced with 500 μM isopropyl-1-thio-β-D-galactopyranoside at 30°C for 4 hours. Cells were harvested by centrifugation and resuspended in

3

lysis buffer [10 mM Tris-HCl pH 7.5, 150 mM NaCl, 1 % (V/V) Triton X-100] containing a protease inhibitor cocktail (Complete mini, Roche. Mannheim, Germany). The protein extract was prepared by sonication, centrifuged and resuspended in the same lysis buffer. This fraction was purified using a Ni-NTA agarose resin (Invitrogen) and eluted with lysis buffer containing 80 mM imidazole.

PI 3-kinase Activity Assays and Substrate Specificity- PI3K activity assays were carried out as described before with some modifications (31). Partially purified recombinant protein (rTcVps34, 0.5 and 5 μg) was assayed in 75 μl reactions containing 20 mM Tris-HCl, pH 7.4, 4 mM $MgCl_2$, 100 mM NaCl, 2 mg.ml^{-1} sonicated phosphatidylinositol, 40 μM ATP and 25 μCi.ml^{-1} γ[^{32}P]-ATP. The mixtures were incubated at 30ºC for 15 min and reactions were terminated by the addition of 150 μl of 1 M HCl. Lipids were extracted first with $CHCl_3$/CH_3OH (1:1) plus 10 mM EDTA and the resulting organic phase was then extracted with CH_3OH/HCl (100:1) plus 10 mM EDTA. The obtained organic phase was dried with nitrogen gas, resuspended in $CHCl_3$/CH_3OH (1:1) and spotted onto LK6D silica gel TLC plate (Whatman, Philadelphia, PA) pre-treated with potassium oxalate and developed with $CHCl_3$/CH_3OH/NH_4OH (40:40:15). Radiolabeled phosphoinositides were detected by autoradiography.

For the substrate specificity experiments, the PI3K activity assays were carried out as described above except that either phosphatidylinositol (PI), phosphatidylinositol-4-phosphate (PI 4-P) or phosphatidylinositol-4,5-bisphosphate (PI 4,5-P_2) were included as substrates (2 mg.ml^{-1}).

For PI3K activity assays using *T. cruzi* epimastigote cell extracts, 25, 50 or 75 μg of total protein were used. After a standard activity reaction as described above, radiolabeled phosphoinositides were measured in a liquid scintillation counter and identified by TLC followed by autoradiography. Unlabeled PI, PI 4-P and PI 4,5-P_2 standards were visualized by staining with iodine vapors.

Parasite Transfection- The full-length *TcVps34* gene was amplified by using the primers PI3K-Fw-pTREX-HindIII   5′ AAGCTTATGACCACCGAAAACGT 3′ and PI3K-Rv-pENTR-XhoI   5′

CTCGAGTTAGTGCCGTGTTGCCTGCGCT 3′ The *TcVps34* gene fused to a His-Tag in the N-terminal was amplified from the construct pDEST17-*TcVps34* by using the primer pDEST17-Fw-HindIII 5′AAGCTTATGTCGTACTACCATCACCATCA 3′ and the same reverse primer PI3K-Rv-pENTR-XhoI. Both 2,724-bp PCR products were then cloned into pGEM-T Easy plasmid and subcloned into the pTREX expression vector, which integrates in the ribosomal locus and allows high expression levels driven by the strong Pol I rRNA promoter in *T. cruzi* (32).

T. cruzi epimastigotes of CL Brener strain were transfected with the pTREX-*TcVps34* and pTREX-His-*TcVps34* constructs as described previously (32). Parasites transfected with a pTREX-GFP construction were monitored by fluorescence microscopy as a selection control. Stable cell lines were achieved after 60 days of treatment with 500 μg.ml^{-1} G418 (Gibco BRL, Carlsbad, CA) and the transgenic condition was confirmed by Southern and western blot analyses.

Differential Interference Contrast and Video Microscopy- Differential interference contrast (DIC) and video microscopy images were taken using an Olympus IX-71 inverted fluorescence microscope with a Photometrix CoolSnapHQ CCD camera driven by DeltaVision software (Applied Precision, Seattle, WA). For analysis of contractile vacuole filling, videomicroscopy of epimastigotes adhered to poly-L-lysine-coated coverslips and bathed in isosmotic buffer was carried out. Videos were recorded for 5 min and reconstructed using the DeltaVision Softworx software. For videomicroscopy of severe hyposmotic treatment, cells were adhered to poly-L-lysine coated coverslips and bathed in 65 mOsm buffer. Videos were recorded for 20 min.

Electron Microscopy- About 1×10^8 epimastigote forms were harvested and washed twice with PBS. The parasites were fixed with freshly prepared 2.5% glutaraldehyde, 4% formaldehyde, 0.1 M sodium cacodylate buffer (pH 7.3) for 1 h and then embedded in epoxy resin, sectioned, and stained using standard methods for transmission electron microscopy. Images were obtained on a Zeiss 900 transmission electron microscope operating at 80 kV. For scanning electron microscopy, cells were fixed as before, adhered to poly-L-lysine-coated coverslips,

4

dehydrated in ethanol series, critical point dried and coated with gold in a Balzers gold sputtering system. Cells were observed in a JEOL JSM 6340F Field Emission Scanning Electron Microscope operating at 5 kV.

Regulatory Volume Decrease- Epimastigotes were collected and washed twice with isotonic chloride buffer (Iso-Cl buffer, 137 mM NaCl, 4 mM KCl, 1.5 mM KH_2PO_4, 8.5 mM Na_2PO_4, 20 mM HEPES, 11 mM glucose, 1 mM $CaCl_2$, 0.8 mM $MgSO_4$, pH 7.4). The osmolarity of the buffer was adjusted to 300 ± 5 mOsm as verified by an Advanced Instruments 3D3 Osmometer (Norwood, MA). The washed cells were resuspended in Iso-Cl buffer to a cell density of 1 x 10^8.ml^{-1} cells. The cells were distributed in 96-well plates with 150 µl per well in triplicate and hyposmotic stress was induced by 1:1 dilution of cell suspension with sterile deionized water, resulting in a final osmolarity of 150 mOsm. The absorbance changes at 550 nm were recorded every 20 s for 10 min using a SpectraMax M2e plate reader (Molecular Devices) (18).

Membrane Integrity and Amino Acid Release- After treatment with the inhibitors wortmannin and LY294,000, membrane integrity was determined by ethidium bromide exclusion as described by Rohloff et al (18). Total amino acid analysis of the cell extracts and the supernatant fraction of epimastigote cells exposed to hypotonic or isotonic buffer were determined as described before (18).

H$^+$ Transport Assays- Active H$^+$ transport was assayed as described previously (33), by measuring changes in the absorbance of acridine orange (493-530 nm) in an OLIS modified SLM-Aminco DW2000 dual-wavelength spectrophotometer. Briefly, for H$^+$-ATPase activity, epimastigotes were incubated at 30°C in a 2.5 ml standard reaction medium containing 125 mM sucrose, 65 mM KCl, 1 mM $MgCl_2$, 10 mM HEPES pH 7.2, 2 mM KH_2PO_4, 450 µM EGTA, 4 µM acridine orange (AO) and 1 µM of digitonin. At the indicated time the reaction was started by adding 1 mM ATP. Bafilomycin A$_1$ and sodium *o*-vanadate were added at 1 µM and 100 µM respectively. For H$^+$-PPase activity, the standard reaction medium contained 130 mM KCl, 10 mM HEPES pH 7.2, 2 mM KH_2PO_4, 450 µM EGTA, 4 µM acridine orange (AO) and 1 µM of digitonin. At the indicated times the reaction was started by

adding 100 µM PPi and the specific inhibitor aminomethylenediphosphonate (AMDP) was added at 100 µM. Each experiment was repeated at least three times with different cell preparations.

Transferrin and Fluid Phase Uptake- For FITC-transferrin (Molecular Probes, Invitrogen) uptake epimastigotes were harvested and washed twice in serum-free LIT medium (sfLIT). The cells were incubated at 28°C for 10 min in sfLIT. FITC-transferrin (50 µg.ml^{-1}) was added, and the cells were further incubated at 28°C for various periods of time. Uptake was stopped by the addition of ice-cold sfLIT and the cells were washed once at 4°C and fixed for 30 min in 4% formaldehyde in PBS. The cells were adhered to slides, mounted, and examined immediately.

Fluid phase uptake was monitored with FITC-BSA (Sigma, Saint Louis, MI). Uptake was performed as described above using 50 µg.ml^{-1} of FITC-BSA.

For fluorescence quantification, the images were taken under non-saturating conditions using identical exposure times. Fluorescence intensity was determined using Data Inspector program of the Delta Vision Restoration System.

RESULTS

Cloning and Characterization of the TcVps34 Gene- A search of *T. cruzi* databases using the *TbVps34* gene from *T. brucei* as query resulted in the identification of an orthologous sequence in this parasite (Tc00.1047053511903.160). Two oligonucleotides designed from this sequence were used to amplify the *T. cruzi* gene using genomic DNA as template. After sequencing *TcVps34*, the 2,724-bp open reading frame was identified. The sequence contained several differences from that reported at the GeneDB database and was therefore annotated at the NCBI under the accession number EU276115[4].

The predicted amino acid sequence of TcVps34 presented the phosphoinositide 3-kinase class III accessory domain (amino acids 318 – 477), which has been suggested to be involved in substrate presentation, and the phosphoinositide 3-kinase catalytic domain (amino acids 513 – 906). In addition, TcVps34 possesses a C2 domain at the N-terminal region (amino acids 97 – 222), which is present in several proteins related to signal transduction (Supplemental data S1). Amino acid

5

sequence analysis showed that TcVps34 has the highest identity (57.4%) with *T. brucei* Vps34 (XP_847451), followed by the *Leishmania major* and *S. cerevisiae* orthologs (35.1% and 25.7%, respectively) (Supplemental data S1). In addition, TcVps34 presented only 27.5% of identity with the human class III PI3K (NP_002638).

TcVps34 Complements a Yeast Vps34-Knockout Strain- To analyze whether the *TcVps34* gene encodes a functional PI3K, the *TcVps34* coding region was subcloned into pYES2 expression vector and used to complement a *S. cerevisiae* Vps34-knockout strain (SEY6210Δ*vps34*::*TRP1*), which possesses a temperature-sensitive phenotype. Expression of *TcVps34* restored the ability of mutant cells to grow at 37ºC, whereas transformation with the empty vector did not, indicating that the *TcVps34* gene encodes a catalytically active PI3K (Fig. 1).

TcVps34 is a Functional Class III Phosphatidylinositol 3-Kinase- The formation of phosphatidylinositol 3-phosphate (PI 3-P) by TcVps34 was tested using the partially-affinity purified recombinant protein (Fig. 2*A*). After a standard PI3K radioactive assay, phosphorylated lipids were resolved by TLC and revealed by autoradiography. The recombinant protein was able to phosphorylate phosphatidylinositol (PI) giving PI 3-P as the major product, as evidenced by the position of the standards run in a borate buffer system (34). The detection of this product was dependent on the protein concentration and was very weak in non-induced *E. coli* extracts (Fig. 2*B*), indicating that endogenous *E. coli* proteins were not responsible for the PI3K activity. In addition, the recombinant TcVps34 substrate specificity was studied using phosphatidylinositol (PI), phosphatidylinositol-4-phosphate (PI 4-P) and phosphatidylinositol-4,5-bisphosphate (PI 4,5-P_2) as substrates. The enzyme only phosphorylated PI producing PI 3-P and was not able to use either PI 4-P or PI 4,5-P_2 as substrate (Fig. 2*C*). These findings, together with the sequence data, led us to conclude that TcVps34 belongs to the class III PI3K family.

TcVps34-overexpressing Epimastigotes Show a Singular Phenotype- Since *Vps34* is essential in other trypanosomatids studied (25), we investigated the phenotypic changes induced by *TcVps34* overexpression. A His-tagged version of the *TcVps34* gene was subcloned into the pTREX integration vector (pTREX-His-*TcVps34*) and transfected into CL Brener epimastigote cells. Stable cell lines were achieved after 60 days of selection in the presence of G418.

Southern blot analysis indicated that *TcVps34* is a single-copy gene. In addition, the presence of an extra copy of *TcVps34*, integrated into the genome of the transfected overexpressing cells, was evidenced as an extra hybridization band (Fig. 3*A*). *TcVps34* expression in the transgenic cells was analyzed by northern and western blot, showing increased levels for the specific mRNA in pTREX-His-*TcVps34*-transfected parasites when compared with wild type CL Brener controls and the presence of the tagged protein only in pTREX-His-*TcVps34*-transfected cells (Fig. 3*B* and *C*). Coomassie blue staining showed equivalent amounts of protein in the P100 and S100 fractions (results not shown). Furthermore, when PI3K activity assays were carried out using 25 and 75 μg of total epimastigote extracts, pTREX-His-*TcVps34*-overexpressing cells showed a 2.5-fold increase when compared to control cells, thus confirming that activity was linearly dependent on protein concentration and overexpression of a functional enzyme (Fig. 3*D*).

Examination of cultures by differential interference contrast (DIC) microscopy (Fig. 4*A*), transmission electron microscopy (TEM; Fig. 4*B*), and video microscopy (Fig. 4*C* and supplemental data S2) revealed striking morphological differences between pTREX-His-*TcVps34*-overexpressing cells and wild type cells. Cells overexpressing His-TcVsp34 showed enlarged contractile vacuoles when compared to wild type cells (Fig. 4*A*). At the electron microscopy level (Fig. 4*B*), contractile vacuoles were visible in most cells overexpressing TcVsp34, whereas this was not the case in wild type cells, as also observed by DIC (Fig. 4*A*). To exclude the possibility that the histidine tag was playing a role in the observed phenotype, transgenic parasites overexpressing the full-length *TcVps34* gene without the tag were generated and their phenotype evaluated as described above for pTREX-His-*TcVps34*. These parasites showed the same morphological alterations when analyzed by DIC and TEM (Fig. 4*A*, right panel and Fig. 4*B* respectively) indicating that these alterations are due to the enhanced expression of *TcVps34*. Moreover, these enlarged organelles were functional, as evidenced

6

by following their periodic filling under video microscopy, when pTREX-His-*TcVps34*-overexpressing epimastigotes were incubated in isosmotic buffer (300 mOsm; Fig. 4*C* and supplemental data S2). Furthermore, most pTREX-His-*TcVps34*- and pTREX-*TcVps34*-overexpressing cells (approximately 95%) displayed a hypertrophic alteration of the plasma membrane between the cytostome and the flagellar pocket, as detected by scanning electron microscopy (SEM, Fig. 5).

Effect of PI 3-kinase Inhibitors on the Regulatory Volume Decrease in Control and pTREX-His-TcVps34-overexpressing Cells- Due to the distinctive phenotype with enlarged contractile vacuoles observed in the pTREX-His-*TcVps34*-overexpressing cells, a possible role for TcVps34 in the adaptation to hyposmotic stress was next investigated. Wild type CL Brener and pTREX-His-*TcVps34*-overexpressing epimastigotes were pre-incubated for 30 min with 3 μM wortmannin or 60 μM LY294,000 and then subjected to hyposmotic stress. Regulatory volume decrease (RVD) was followed by light scattering and compared with untreated controls. These inhibitors considerably reduced the RVD in wild type cells, whereas they had no effect on pTREX-His-*TcVps34*-overexpressing parasites (Fig. 6*A* and *B*). To exclude the possibility of toxic side effects due to the treatment with the inhibitors, we confirmed that the plasma membrane remained intact and that the hyposmotically induced amino acid efflux was not affected (data not shown). Since overexpression of *TcVps34* could be limiting the effects of the PI3K inhibitors with other possibly present lipid kinases that these inhibitors can affect, we investigated the lipid kinase activity in wild type and pTREX-His-*TcVps34*-overexpressing parasites in the presence of 3 μM wortmannin and 60 μM LY294,000. Similarly, we observed that both compounds inhibited the lipid kinase activity in wild type cells (41 and 30 % approximately for wortmannin and LY294,000 respectively) whereas they had a minor effect in pTREX-His-*TcVps34*-overexpressing parasites (9 and 5 % approximately for wortmannin and LY294,000 respectively). Videomicroscopy of both pTREX-*TcVps34*- and pTREX-His-*TcVps34*-overexpressing epimastigotes submitted to severe hyposmotic stress (65 mOsm) showed that, in contrast to wild type cells, after 20 min incubation, *TcVps34*-overexpressing cells were able to recover their original volume (Fig. 6*C*, supplemental data S3, S4 and S5). Taken together, these results suggest an active role for TcVps34 in the parasite response to hyposmotic stress. It is important to remark that no differences were observed when wild type cells were compared with those transfected with the pTREX-GFP vector (data not shown).

H^+-ATPase and H^+-PPase Activities in pTREX-His-*TcVps34-overexpressing Cells-* It has been reported that in *Candida albicans*, Vps34p interacts with Vma7p, a subunit of the vacuolar H^+-ATPase. In addition, *C. albicans Vps34*-null mutants show vacuolar acidification defects, as a result of a defective proton transport into the vacuole, due to the lack of Vps34p-Vma7p interaction (35). In order to investigate the influence of TcVps34 in intracellular acidification, we studied the H^+-ATPase and H^+-PPase activities in pTREX-His-*TcVps34*-overexpressing cells. In this assay, vesicle acidification induced by ATP or pyrophosphate (PPi) was measured as the decrease in absorbance of acridine orange at 493-530 nm in permeabilized parasites (33). Results showed that ATP-dependent proton uptake was higher in pTREX-His-*TcVps34*-overexpressing cells (Fig. 7, trace b) than in wild type cells (Fig. 7, trace a). This activity was strongly inhibited by 1 μM of bafilomycin A$_1$, a specific inhibitor of the vacuolar-type H^+-ATPases (36) (Fig. 7*A*), and less affected by 100 μM of sodium *o*-vanadate, an inhibitor of P-type H^+-ATPases (37) (Fig. 7*B*). This suggests that proton transport by intracellular compartments in both wild type and pTREX-His-*TcVps34*-overexpressing cells is mainly achieved by the vacuolar-type H^+-ATPase. Interestingly, in contrast to that observed for ATP-driven proton uptake, PPi-dependent proton transport was higher in wild type cells (Fig. 7*C*, trace a) than in pTREX-His-*TcVps34*-overexpressing cells (Fig. 7*C*, trace b). This transport was strongly inhibited by 100 μM of aminomethylenediphosphonate (AMDP), a pyrophosphate analog that specifically inhibits vacuolar proton pyrophosphatases (38) (Fig. 7*C*). These results indicate that overexpression of *TcVps34* produces alterations in vesicle acidification, and suggest that changes in acidification mediated by these two pumps might be coordinated. In all experiments, proton gradient

was collapsed and intraorganellar pH was neutralized with the addition of 1 μM of the K$^+$/H$^+$ ionophore nigericin.

Receptor-Mediated and Fluid Phase Endocytosis in pTREX-His-TcVps34-overexpressing Cells- To study whether TcVps34 participates in the endocytic pathway, fluid phase uptake of BSA and receptor-mediated endocytosis of transferrin were analyzed and quantified by fluorescence microscopy. Uptake of the fluid phase marker FITC-BSA was not affected in pTREX-His-*TcVps34*-overexpressing cells when compared with wild type parasites (data not shown). However, receptor-mediated endocytosis measured with FITC-transferrin was significantly blocked in pTREX-His-*TcVps34*-overexpressing cells observed at 10 and 30 min (Fig. 8*A* and *B*, respectively). Quantification of fluorescence indicates an important reduction of internalized transferrin in pTREX-His-*TcVps34*-overexpressing cells ($p < 0.0001$) (Table 1). These results suggest that TcVps34 is involved mainly in the transport of cargo taken up by receptor-mediated endocytosis to the lysosome, and they are in agreement with previous observations reported for other lower eukaryotic cells such as *T. brucei* and *S. cerevisiae* (23,25).

DISCUSSION

Little is known about the response mechanisms that allow survival of trypanosomatids when subjected to the environmental changes that occur throughout their life cycles. A very important aspect is their capacity to adapt to different osmotic conditions. A previous work has demonstrated a relationship between the regulatory volume decrease (RVD) that occurs after hyposmotic stress and the cAMP signaling pathway (20). More recently, we characterized a membrane-associated cAMP-specific phosphodiesterase that possesses a FYVE domain, which is known to bind to membranes enriched in PI 3-P and whose activity is modulated by the same inhibitors that affect RVD during the hyposmotic stress (39). These results led us to investigate the importance of PI 3-P production in the osmoregulation of trypanosomatids.

In this work, we characterized TcVps34, the first Class III PI3K described in *T. cruzi*, and found that this PI3K participates in receptor-mediated endocytosis and osmoregulation in this parasite. *TcVps34* is a single-copy gene and shares a high degree of similarity with its mammalian, *S. cerevisiae,* and *T. brucei* orthologs. Moreover, its protein sequence conserves the Class III PI3K domain structure, with an N-terminal C2 domain, an accessory domain, and a C-terminal kinase domain. The enzyme is functional as indicated by the reversion of the thermosensitive phenotype of a *S. cerevisiae Vps34*-knockout strain. We also demonstrated that the recombinant protein exclusively phosphorylated PI to produce PI 3-P, supporting our analysis that TcVps34 belongs to the group of Class III PI3Ks.

TcVps34 overexpression in epimastigotes produced distinctive morphological and functional changes related to membrane trafficking. The presence of enlarged and functional contractile vacuoles was evident in most *TcVps34*-overexpressing parasites. In addition, some of these cells showed hypertrophic alterations in the region near the cytostome and the flagellar pocket. This phenotype could be originated by a higher membrane trafficking from the enlarged contractile vacuole to these sites, where *T. cruzi* exchanges material with the environment (40). Furthermore, pre-incubation of non-transfected epimastigotes with the PI3K inhibitors wortmannin or LY294,000 reduced the regulatory volume decrease of the parasites subjected to hyposmotic stress. Previous studies have shown that the physiological increase in cell volume is a potent stimulus for Class I PI3K activation (41,42); however, there is little information about the activation of Class III PI3Ks under hyposmotic stress. Although wortmannin and LY294,000 inhibit all PI3Ks to some extent, the observation that plants (43) possess only one Class III PI3K and *S. cerevisiae* (44) and *T. brucei* (25) possess only one genuine PI3K that appears to be Class III by sequence comparison, together with our analysis of the *T. cruzi* genome, supports the idea that the observed effects are related to the inhibition of TcVps34. We conclude that TcVps34 has therefore a role in osmoregulation. It is interesting to note that Braga et al. (45) have reported that epimastigotes of *T. cruzi* (Y strain) treated with wortmannin also show morphological alterations in the flagellar pocket and membrane detachment from the flagellum. These observations might indicate a connection between

8

TcVps34 and membrane trafficking, since the flagellar pocket together with the cytostome are the main sites where this process takes place in trypanosomatids (40,46). Similar observations have been made upon knockdown of *TbVps34* expression by RNA interference in *T. brucei* (25).

A previous work has demonstrated that antibodies against human Vps34 (hVps34) interfere with sorting of endocytosed PDGF receptors and weakly inhibit transferrin recycling (47). Furthermore, the existence of an alternative recycling pathway dependent on PI3K activity has been reported (48). In this regard, our results indicate that fluid phase endocytosis is not affected in pTREX-His-*TcVps34*-overexpressing cells, but that, surprisingly, as it occurs after the knockdown of *TbVps34* in *T. brucei*, overexpression of *TcVps34* in *T. cruzi* produces a blockage of receptor-mediated endocytosis. This could be due to a possible down-regulation of the endocytic pathway, to a defect in recycling of surface receptors, or to a dominant negative effect of the overexpressed protein. Furthermore, in mammalian cells it has been described that PI3K activity regulates the sorting of the EGF receptor, whereas the transport of fluid phase markers remains unaffected (49).

Recently, the interaction of Vps34p and a subunit of the vacuolar-type H^+-ATPase has been reported in *C. albicans* (35). In addition, *C. albicans vps34*-null mutants show acidification defects (31). Therefore, the functional data obtained in this organism resemble the alterations observed in pTREX-His-*TcVps34*-overexpressing epimastigotes, although the hypothesis of an interaction of TcVps34 and *T. cruzi* vacuolar-type H^+-ATPase remains to be investigated. Interestingly, the observation that pTREX-His-*TcVps34*-overexpressing cells showed higher V-H^+-ATPase and lower H^+-PPase activities than wild type parasites suggests that both pumps might be coordinated in order to regulate the pH levels of intracellular compartments.

It is worth mentioning that in *T. cruzi* both V-type H^+-ATPase and H^+-PPase localize to the acidocalcisomes among other cellular locations (19,36,38). Acidocalcisomes are acidic calcium-containing organelles that, together with the contractile vacuole, play a very important role in osmoregulation in *T. cruzi* (20). This might suggest that the alterations in osmoregulation observed in the presence of PI3K inhibitors could be linked to the defects in proton uptake in the pTREX-His-*TcVps34*-overexpressing cells. In contrast, H^+ uptake was poorly affected by vanadate, a specific inhibitor of the P-type H^+-ATPase, which is mainly localized in reservosomes (50), thus suggesting that this pump is scarcely altered by *TcVps34* overexpression.

In summary, the present work provides the first evidence for the presence of a Class III PI3K in *T. cruzi,* and describes its role in osmoregulation. Our results also suggest a role for TcVps34 in protein trafficking and vesicle acidification as it occurs with its orthologs in other organisms (Fig. 9). The unique features of *T. cruzi* vesicular trafficking lead us to propose that this pathway could provide promising targets for the chemotherapy of Chagas' disease.

REFERENCES

1.   Fry, M. J. (1994) *Biochim Biophys Acta* **1226**, 237-268
2.   Katso, R., Okkenhaug, K., Ahmadi, K., White, S., Timms, J., and Waterfield, M. D. (2001) *Annu Rev Cell Dev Biol* **17**, 615-675
3.   Hiles, I. D., Otsu, M., Volinia, S., Fry, M. J., Gout, I., Dhand, R., Panayotou, G., Ruiz-Larrea, F., Thompson, A., Totty, N. F., and et al. (1992) *Cell* **70**, 419-429
4.   Martin, T. F. (1998) *Annu Rev Cell Dev Biol* **14**, 231-264
5.   Fruman, D. A., Meyers, R. E., and Cantley, L. C. (1998) *Annu Rev Biochem* **67**, 481-507
6.   Vanhaesebroeck, B., and Waterfield, M. D. (1999) *Exp Cell Res* **253**, 239-254
7.   Brown, R. A., and Shepherd, P. R. (2001) *Biochem Soc Trans* **29**, 535-537
8.   Gaidarov, I., Smith, M. E., Domin, J., and Keen, J. H. (2001) *Mol Cell* **7**, 443-449
9.   Schu, P. V., Takegawa, K., Fry, M. J., Stack, J. H., Waterfield, M. D., and Emr, S. D. (1993) *Science* **260**, 88-91

10.   Burda, P., Padilla, S. M., Sarkar, S., and Emr, S. D. (2002) *J Cell Sci* **115**, 3889-3900
11.   Eck, R., Bruckmann, A., Wetzker, R., and Kunkel, W. (2000) *Yeast* **16**, 933-944
12.   Petiot, A., Ogier-Denis, E., Blommaart, E. F., Meijer, A. J., and Codogno, P. (2000) *J Biol Chem* **275**, 992-998
13.   Rog, O., Smolikov, S., Krauskopf, A., and Kupiec, M. (2005) *Curr Genet* **47**, 18-28
14.   Stack, J. H., Horazdovsky, B., and Emr, S. D. (1995) *Annu Rev Cell Dev Biol* **11**, 1-33
15.   Guhl, F., and Lazdins-Helds, J. (2007) Report of the Scientific Working Group on Chagas disease, Buenos Aires, Argentina 17-20 April 2005, *World Health Organization*
16.   Kollien, A. H., Grospietsch, T., Kleffmann, T., Zerbst-Boroffka, I., and Schaub, G. A. (2001) *J Insect Physiol* **47**, 739-747
17.   Rohloff, P., and Docampo, R. (2008) *Exp Parasitol* **118**, 17-24
18.   Rohloff, P., Rodrigues, C. O., and Docampo, R. (2003) *Mol Biochem Parasitol* **126**, 219-230
19.   Montalvetti, A., Rohloff, P., and Docampo, R. (2004) *J Biol Chem* **279**, 38673-38682
20.   Rohloff, P., Montalvetti, A., and Docampo, R. (2004) *J Biol Chem* **279**, 52270-52281
21.   Alonso, G. D., Schoijet, A. C., Torres, H. N., and Flawia, M. M. (2006) *Mol Biochem Parasitol* **145**, 40-49
22.   Corvera, S. (2001) *Traffic* **2**, 859-866
23.   Simonsen, A., Wurmser, A. E., Emr, S. D., and Stenmark, H. (2001) *Curr Opin Cell Biol* **13**, 485-492
24.   Wishart, M. J., Taylor, G. S., and Dixon, J. E. (2001) *Cell* **105**, 817-820
25.   Hall, B. S., Gabernet-Castello, C., Voak, A., Goulding, D., Natesan, S. K., and Field, M. C. (2006) *J Biol Chem* **281**, 27600-27612
26.   Kihara, A., Noda, T., Ishihara, N., and Ohsumi, Y. (2001) *J Cell Biol* **152**, 519-530
27.   Pereira, C. A., Alonso, G. D., Paveto, M. C., Iribarren, A., Cabanas, M. L., Torres, H. N., and Flawia, M. M. (2000) *J Biol Chem* **275**, 1495-1501
28.   Alonso, G. D., Schoijet, A. C., Torres, H. N., and Flawia, M. M. (2007) *Mol Biochem Parasitol* **152**, 72-79
29.   Laemmli, U. K. (1970) *Nature* **227**, 680-685
30.   Gietz, R. D., and Schiestl, R. H. (1991) *Yeast* **7**, 253-263
31.   Gunther, J., Nguyen, M., Hartl, A., Kunkel, W., Zipfel, P. F., and Eck, R. (2005) *Microbiology* **151**, 81-89
32.   Vazquez, M. P., and Levin, M. J. (1999) *Gene* **239**, 217-225
33.   Scott, D. A., de Souza, W., Benchimol, M., Zhong, L., Lu, H. G., Moreno, S. N., and Docampo, R. (1998) *J Biol Chem* **273**, 22151-22158
34.   Ono, F., Nakagawa, T., Saito, S., Owada, Y., Sakagami, H., Goto, K., Suzuki, M., Matsuno, S., and Kondo, H. (1998) *J Biol Chem* **273**, 7731-7736
35.   Eck, R., Nguyen, M., Gunther, J., Kunkel, W., and Zipfel, P. F. (2005) *Int J Med Microbiol* **295**, 57-66
36.   Benchimol, M., De Souza, W., Vanderheyden, N., Zhong, L., Lu, H. G., Moreno, S. N., and Docampo, R. (1998) *Biochem J* **332 (Pt 3)**, 695-702
37.   Scott, D. A., and Docampo, R. (1998) *Biochem J* **331 (Pt 2)**, 583-589
38.   Martinez, R., Wang, Y., Benaim, G., Benchimol, M., de Souza, W., Scott, D. A., and Docampo, R. (2002) *Mol Biochem Parasitol* **120**, 205-213
39.   Seet, L. F., and Hong, W. (2001) *J Biol Chem* **276**, 42445-42454
40.   Soares, M. J. (2006) *Parasitol Res* **99**, 321-322

41.	Feranchak, A. P., Roman, R. M., Schwiebert, E. M., and Fitz, J. G. (1998) *J Biol Chem* **273**, 14906-14911

42.	Van der Kaay, J., Beck, M., Gray, A., and Downes, C. P. (1999) *J Biol Chem* **274**, 35963-35968

43.	Mueller-Roeber, B., and Pical, C. (2002) *Plant Physiol* **130**, 22-46

44.	Foster, F. M., Traer, C. J., Abraham, S. M., and Fry, M. J. (2003) *J Cell Sci* **116**, 3037-3040

45.	Braga, M. V., and de Souza, W. (2006) *FEMS Microbiol Lett* **256**, 209-216

46.	Porto-Carreiro, I., Attias, M., Miranda, K., De Souza, W., and Cunha-e-Silva, N. (2000) *Eur J Cell Biol* **79**, 858-869

47.	Siddhanta, U., McIlroy, J., Shah, A., Zhang, Y., and Backer, J. M. (1998) *J Cell Biol* **143**, 1647-1659

48.	van Dam, E. M., Ten Broeke, T., Jansen, K., Spijkers, P., and Stoorvogel, W. (2002) *J Biol Chem* **277**, 48876-48883

49.	Petiot, A., Faure, J., Stenmark, H., and Gruenberg, J. (2003) *J Cell Biol* **162**, 971-979

50.	Vieira, M., Rohloff, P., Luo, S., Cunha-e-Silva, N. L., de Souza, W., and Docampo, R. (2005) *Biochem J* **392**, 467-474

FOOTNOTES

[1]To whom correspondence may be addressed: Center for Tropical and Emerging Global Diseases and Department of Cellular Biology, University of Georgia, Athens, GA 30602, USA. Tel: 706-542-8104; Fax: 706-542-9493; e-mail: rdocampo@uga.edu.

[2]To whom correspondence may be addressed: Instituto de Investigaciones en Ingeniería Genética y Biología Molecular (INGEBI-CONICET). Vuelta de Obligado 2490 (1428), Buenos Aires, Argentina. Tel: 54-11-4783-2871; Fax: 54-11-4786-8578; e-mail: galonso@dna.uba.ar.

[3]The abbreviations used are: PI, phosphatidylinositol; PI 3-P, phosphatidylinositol 3-phosphate; PI 4-P, phosphatidylinositol 4-phosphate; PI 4,5-P_2, phosphatidylinositol 4,5-bisphosphate; PI3K, phosphatidylinositol 3-kinase; Vps , vacuolar protein sorting; TLC, thin layer chromatography; RVD, regulatory volume decrease; FYVE, (Fab-1, YGL023, Vps27, and EEA1); AMDP, aminomethylenediphosphonate; DIC, differential interference contrast; PDGF, platelet-derived growth factor; EGF, epidermal growth factor.

[4]Nucleotide sequence data reported in this paper are available in the GenBank™ database under the accession number EU276115.

FIGURE LEGENDS

FIGURE 1. Complementation of a yeast *Vps34*-knockout strain. The temperature-sensitive Δ*vps34*::*TRP1* strain SEY6210 was transformed with either the pYES2 empty vector (pYES) or with the same plasmid carrying the full-length *TcVps34* gene (pYES-*TcVps34*). Several dilutions were plated into synthetic selective media (without tryptophan and uracil) and grown for 72 h at 37ºC.

FIGURE 2. Lipid kinase activity of recombinant TcVps34. (*A*) The His-tagged TcVps34 recombinant protein was affinity purified from the soluble fraction of IPTG-induced *E. coli* BL21(DE3) using a Ni-NTA agarose resin and samples were examined by SDS-PAGE (Coomassie Blue-stained). *Lane 1*: non-induced soluble fraction; *lane 2*: induced soluble fraction; *lane 3*: molecular weight marker; *lane 4*: flow-through; *lane 5*: wash; *lanes 6*, *7*, *8* and *9*: elutions with 40, 80, 250 and 500 mM imidazole respectively. Lane 1 and Lane 2 were loaded with the same amount of protein. (*B*) The 80 mM elution fraction of the His-tagged recombinant TcVps34 was incubated with $\gamma[^{32}P]$-ATP and phosphatidylinositol. After incubation with the indicated amounts of protein, the reaction products were separated by TLC and labeled lipids were detected by autoradiography. The main product, phosphatidylinositol 3-phosphate (PI 3-P); the migration of standards: phosphatidylinositol (PI), phosphatidylinositol 4-phosphate (PI 4-P), phosphatidylinositol-4,5-bisphosphate (PI 4,5-P_2) and the Origin are identified by arrows. (*C*) For substrate specificity, PI3K assays were performed as above in the presence of phosphatidylinositol (PI), phosphatidylinositol-4-phosphate (PI 4-P) and phosphatidylinositol-4,5-bisphosphate (PI 4,5-P_2) as substrates. Phosphatidylinositol 3-phosphate (PI 3-P); the migration of standards: phosphatidylinositol (PI), phosphatidylinositol 4-phosphate (PI 4-P), phosphatidylinositol-4,5-bisphosphate (PI 4,5-P_2) and the Origin are identified by arrows.

FIGURE 3. Molecular analysis of pTREX-His-*TcVps34*-transfected cells. (*A*) Southern blot analysis of wild type and pTREX-His-*TcVps34*-transfected parasites. Total genomic DNA (5 µg) was digested with the restriction enzymes NsiI, BanI, SacII (which cut in the positions 735, 639 and 592 of *TcVps34* respectively) and HindIII (which cuts the position 1041 of the *TcVps34* gene); electrophoresed; blotted and hybridized with a probe corresponding to the first 990-bp of the *TcVps34* coding region. (*B*) Northern blot analysis of wild type and pTREX-His-*TcVps34*-transfected parasites. Total RNA (30 µg) from wild type or pTREX-His-*TcVps34*-transfected parasites was electrophoresed in agarose-formaldehyde gels, blotted and hybridized with the same probe described above. The migration position and loading control corresponding to the three ribosomal RNA bands are indicated. (*C*) Western blot analysis of wild type and transfected parasites. Western blot were performed using soluble (S100) or membrane (P100) fractions (80 µg) from wild type (WT) or pTREX-His-*TcVps34*-transfected parasites (His-TcVps34) and the recombinant protein (Rec) purified from *E. coli* (5 µg) as control; resolved by SDS-PAGE (8% gels); electrotransferred on to Hybond C membranes and revealed with an anti-6-His antibody. (*D*) Enhanced PI3K activity in pTREX-His-*TcVps34*-transfected parasites. PI3K activity assays were performed as described under Experimental Procedures using 25 and 75 µg of wild type (WT) and pTREX-His-*TcVps34* (His-TcVps34) total parasite extracts. Bars represent the standard deviation of duplicates.

FIGURE 4. Overexpression of *TcVps34* in *T. cruzi* epimastigote cells causes morphological alterations. (*A*) Transgenic wild type, pTREX-His-*TcVps34*- and pTREX-*TcVps34*-overexpressing cells were adhered to poly-L-lysine coverslips, bathed in isosmotic buffer and examined by differential interference contrast microscopy. Arrows show large contractile vacuoles. Note the absence of a large and visible vacuole in the wild type cells. (*B*) Transmission electron microscopy of pTREX-His-*TcVps34*- and pTREX-*TcVps34*-overexpressing cells (His-TcVps34 and TcVps34 respectively). Arrows show large contractile vacuoles and arrowheads show acidocalcisomes containing electron-dense material near the contractile vacuole membrane. Flagellar pocket is indicated as FP. (*C*) Video microscopy of contractile vacuole filling and emptying in pTREX-His-*TcVps34*-overexpressing cells. The cells were treated as in "(*A*)", video microscopy data were collected, and selected frames are shown. Numbers in each frame indicate the time lapse. Arrows show the position of the contractile vacuole.

FIGURE 5. *TcVps34*-overexpressing epimastigotes show morphological alterations in the plasma membrane region between the cytostome and the flagellar pocket. Field emission scanning electron microscopy revealed swelling of the plasma membrane region between the cytostome and the flagellar pocket (arrow) in pTREX-His-*TcVps34*-overexpressing cells (*A*) when compared to wild type cells (**inset in *A***). The same phenotype was observed in pTREX-*TcVps34*-overexpressing parasites (non-tagged overexpressing cells, panel *B*). Panel *C* and *D* show magnifications of the regions indicated by squares in panel *B*.

FIGURE 6. Effect of PI 3-kinase inhibitors on regulatory volume decrease. Wild type (*A*) and transfected pTREX-His-*TcVps34*-overexpressing cells (*B*) were pre-incubated with either 3 μM wortmannin (*triangles*) or 60 μM LY294,000 (*squares*), and then subjected to hyposmotic stress. Volume recovery compared with untreated controls (*circles*) was followed by light scattering. Results are representative of those obtained from at least three independent experiments. (*C*) Time lapse snapshots of wild type (WT) and transfected pTREX-His-*TcVps34*-overexpressing cells (TcVps34) subjected to 65 mOsm hyposmotic stress. Note that in contrast to WT cells, pTREX-His-*TcVps34*-overexpressing cells were able to recover their original volume.

FIGURE 7. H^+-ATPase and H^+-PPase activities. Acridine orange uptake assay conditions were as described under Experimental Procedures. (*A*) *trace a*, wild type cells, no additions; *trace b*, pTREX-His-*TcVps34*-overexpressing cells, no additions; *trace c*, wild type cells plus 1 μM bafilomycin A_1 (BAF); *trace d*, pTREX-His-*TcVps34*-overexpressing cells plus 1 μM bafilomycin A_1. (*B*) *Trace a*, wild type cells, no additions; *trace b*, pTREX-His-*TcVps34*-overexpressing cells, no additions; *trace c*, wild type cells plus 100 μM sodium *o*-vanadate (VAN); *trace d*, pTREX-His-*TcVps34*-overexpressing cells plus 100 μM sodium *o*-vanadate. (*C*) *Trace a*, wild type cells, no additions; *trace b*, pTREX-His-*TcVps34*-overexpressing cells, no additions; *trace c*, wild type cells plus 100 μM AMDP; *trace d*, pTREX-His-*TcVps34*-overexpressing cells plus 100 μM AMDP. In all cases, the pH gradient was collapsed after addition of 1 μM nigericin (NIG). Results are representative of those obtained from at least three independent experiments with different cell preparations. Addition of the substrates (ATP and PPi) and specific inhibitors (BAF, VAN and AMDP) are indicated by arrows.

FIGURE 8. pTREX-His-*TcVps34*-overexpressing epimastigote cells specifically show reduced receptor-mediated endocytosis of FITC-transferrin. Wild type and pTREX-His-*TcVps34*-overexpressing cells were incubated for 10 min (*A*) and 30 min (*B*) with FITC-transferrin. Cells were fixed in 4% formaldehyde, adhered to poly-L-lysine slides and examined immediately by differential interference contrast and fluorescence microscopy. *Bar*: 6.7 μm.

FIGURE 9. Multiple roles for TcVps34. Schematic representation of the pathways in which TcVps34 is involved. TcVps34 plays a role in osmoregulation, and on this basis the PI3K inhibitors wortmannin and LY294,000 reduce the RVD of epimastigotes subjected to hyposmotic stress, resulting in a less water movement outside the cell by the contractile vacuole complex (CV) (I). In addition, TcVps34 is implicated in vesicle acidification, as suggested by the changes in the activities of the V-H^+-ATPase and the V-H^+-PPase proton pumps localized in the acidocalcisomes (Ac) after its overexpression (II). Finally, TcVps34 is involved in membrane trafficking, which is evidenced by a decrease in receptor-mediated endocytosis in cells overexpressing this enzyme (III).

Supplemental data S1. Alignment of the full-length sequences corresponding to TcVps34 (accession number ABX71159); phosphatidylinositol 3-kinase, putative from *Trypanosoma brucei* (accession number XP_847451); phosphatidylinositol 3-kinase, putative [*Leishmania major*] (accession number XP_001683719) and phosphatidylinositol 3-kinase [*Saccharomyces cerevisiae*] (accession number

13

NP_013341). The C2 domain (amino acids 97 – 222), phosphoinositide 3-kinase class III accessory domain (amino acids 318 – 477), and phosphoinositide 3-kinase catalytic domain (amino acids 513 – 906) are denoted by dotted, dashed and solid lines over the sequences, respectively. The numbers indicated above are according to the amino acid positions of the TcVps34. Sequences were aligned using the ClustalW program and edited with BOXSHADE (3.33c) software. Amino acids are colored as follows: white for different residues, black for identical residues, gray for similar and conserved residues.

Supplemental data S2. Videomicroscopy of contractile vacuole filling and emptying. pTREX-His-*TcVps34*-overexpressing parasites were adhered to poly-L-lysine coverslips, bathed in isosmotic (300 mOsm) buffer and the contractile vacuole filling and emptying cycles recorded.

Supplemental data S3. Response to severe hyposmotic treatment of wild type epimastigote cells. Parasites were adhered to poly-L-lisine coverslips, bathed in severe hyposmotic (65 mOsm) buffer and videos recorded for 20 min.

Supplemental data S4. Response to severe hyposmotic treatment of pTREX-His-*TcVps34*-overexpressing parasites. Cells were adhered to poly-L-lisine coverslips, bathed in severe hyposmotic (65 mOsm) buffer and videos recorded for 20 min.

Supplemental data S5. Response to severe hyposmotic treatment of pTREX-*TcVps34*-overexpressing parasites. Cells were adhered to poly-L-lisine coverslips, bathed in severe hyposmotic (65 mOsm) buffer and videos recorded for 20 min.

Table 1. Quantification of receptor-mediated endocytosis of FITC-transferrin. Fluorescence intensity of FITC-transferrin uptake was quantified as described under Experimental Procedures. The values represent the mean fluorescence (arbitrary units) of at least 60 cells for each condition.

Time (min)	FITC-transferrin fluorescence in wild type cells	FITC-transferrin fluorescence in pTREX-His-*TcVps34*-overexpressing cells	% endocytosis inhibition
10	565.20 ± 120.94	242.06 ± 55.85	55.85
30	658.94 ± 150.93	278.89 ± 63.65	57.67

Figure 1
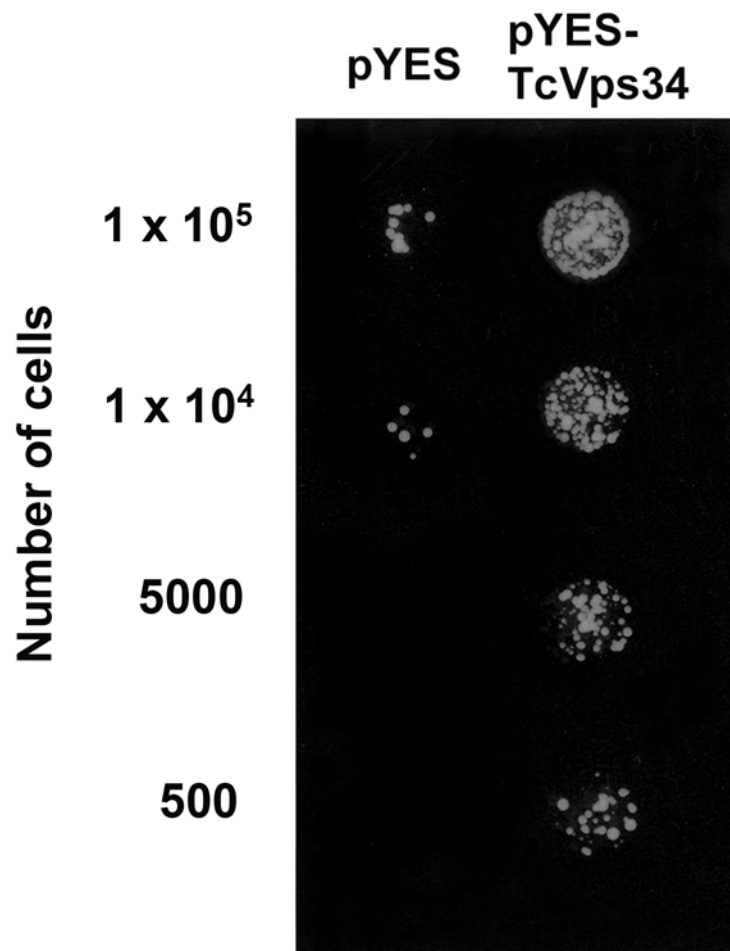
Figure 2

Figure 3

Figure 4

19

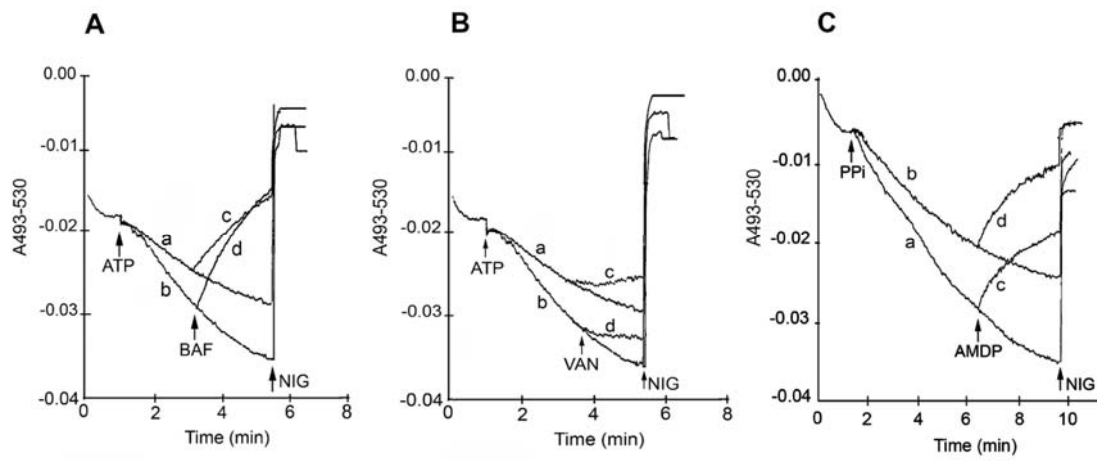**Figure 5**

Figure 6

21
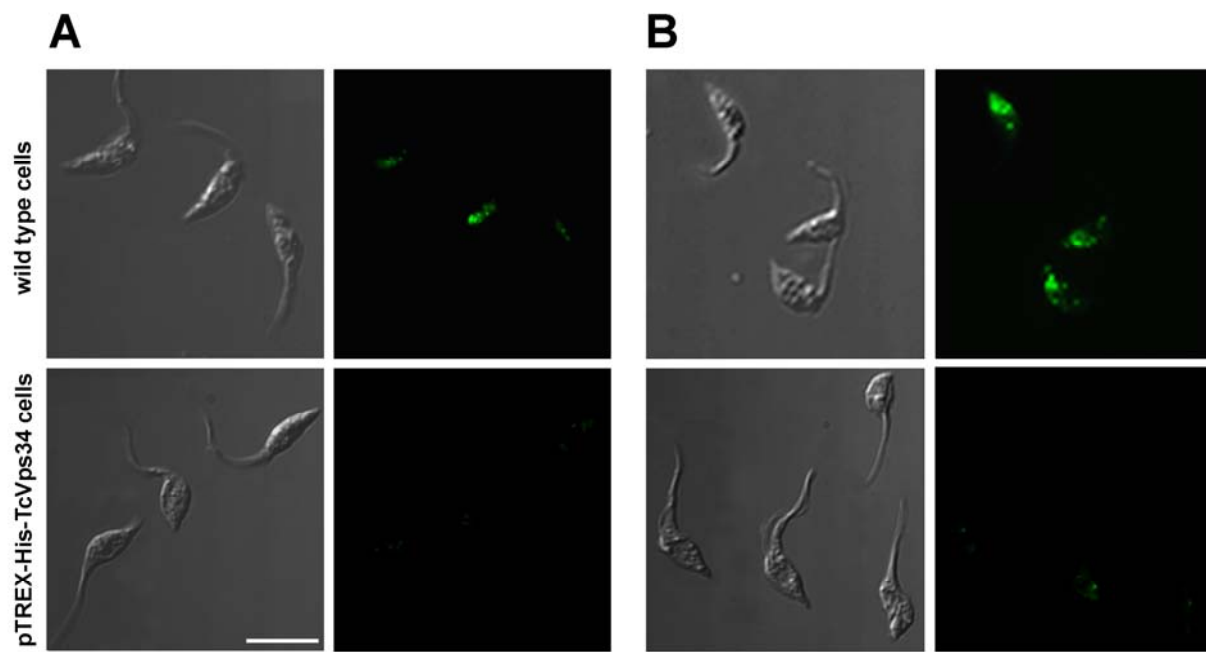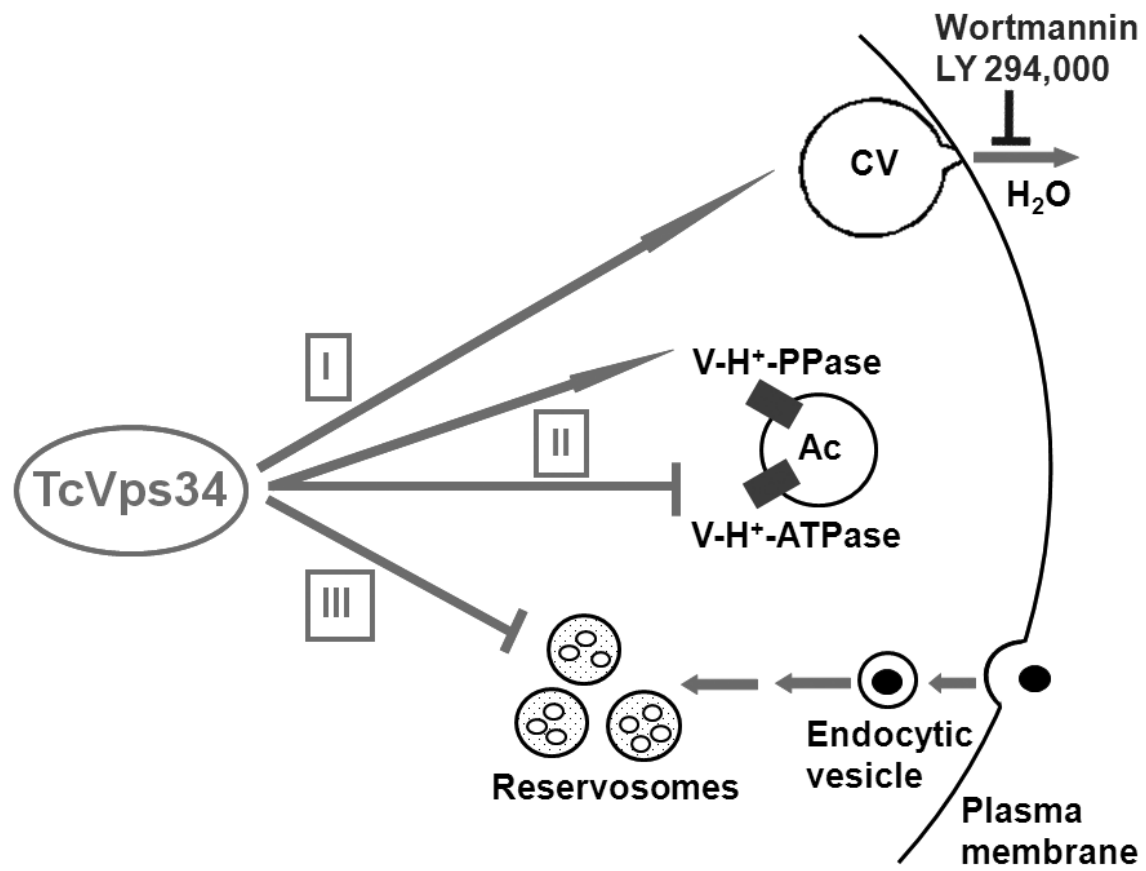
Figure 7

22
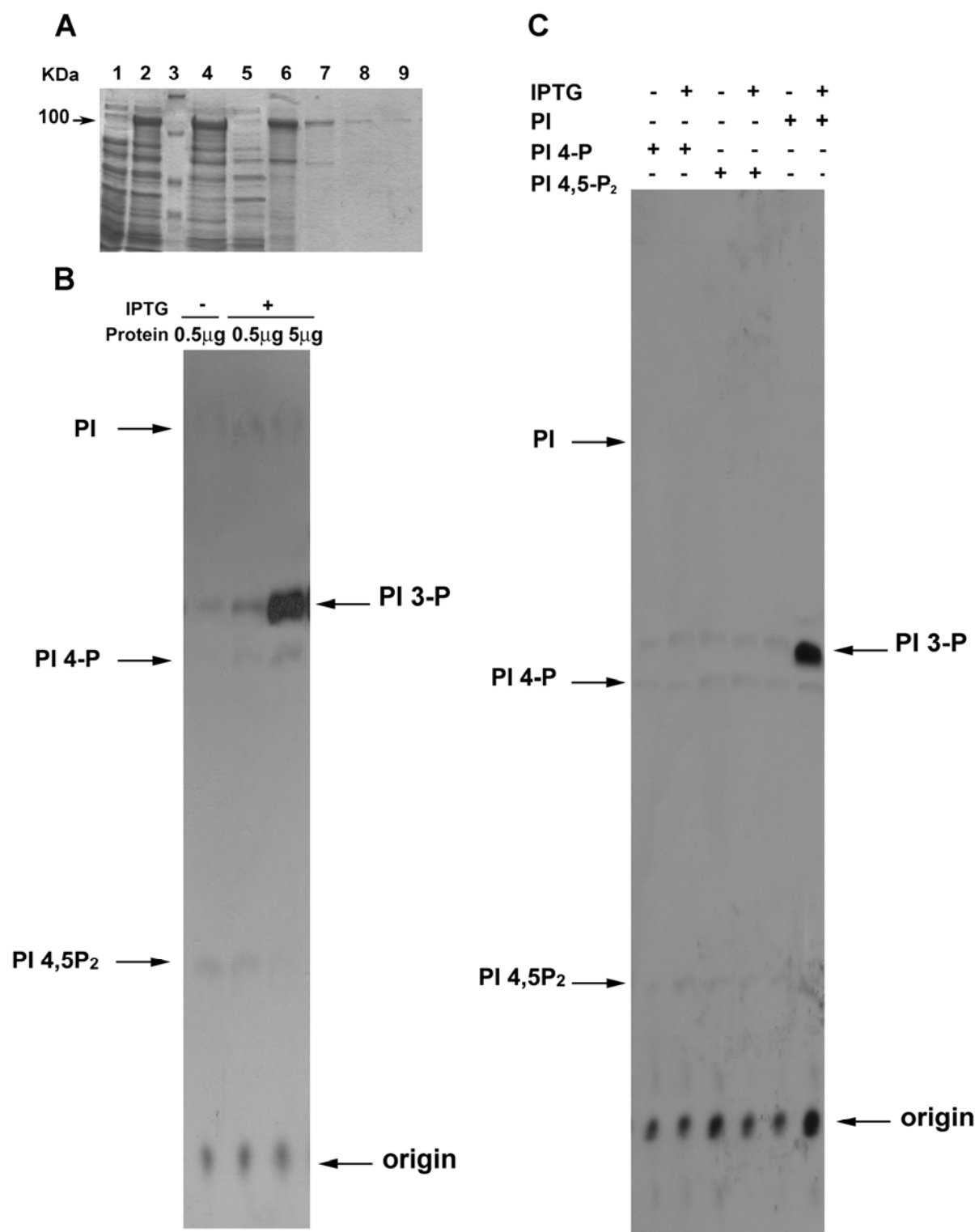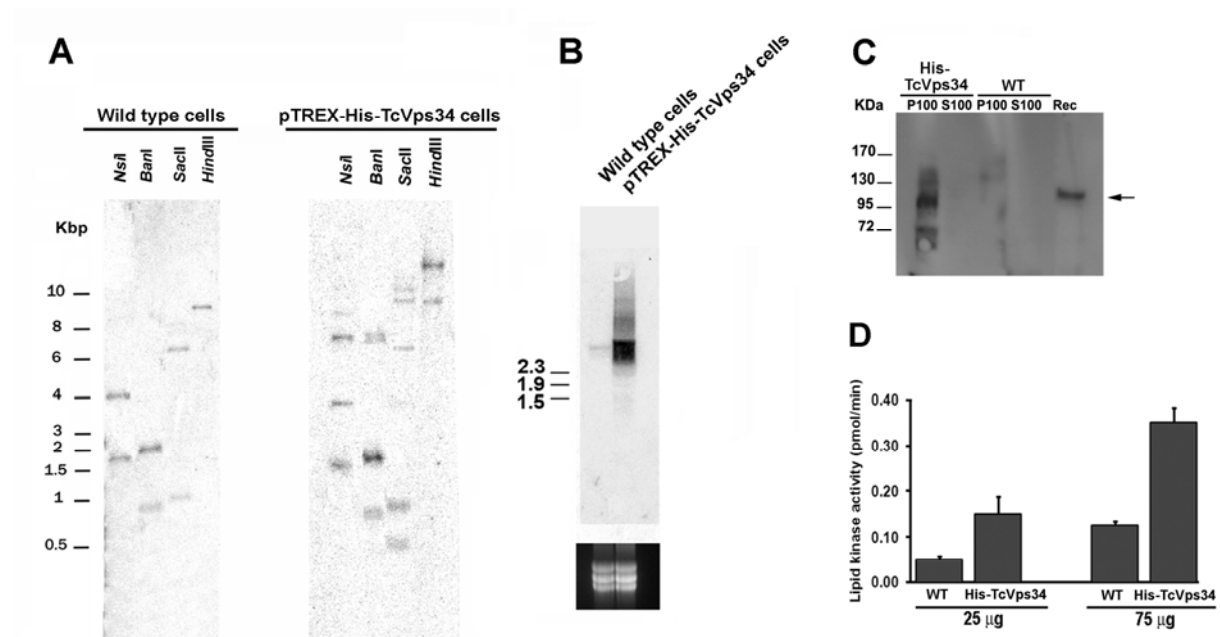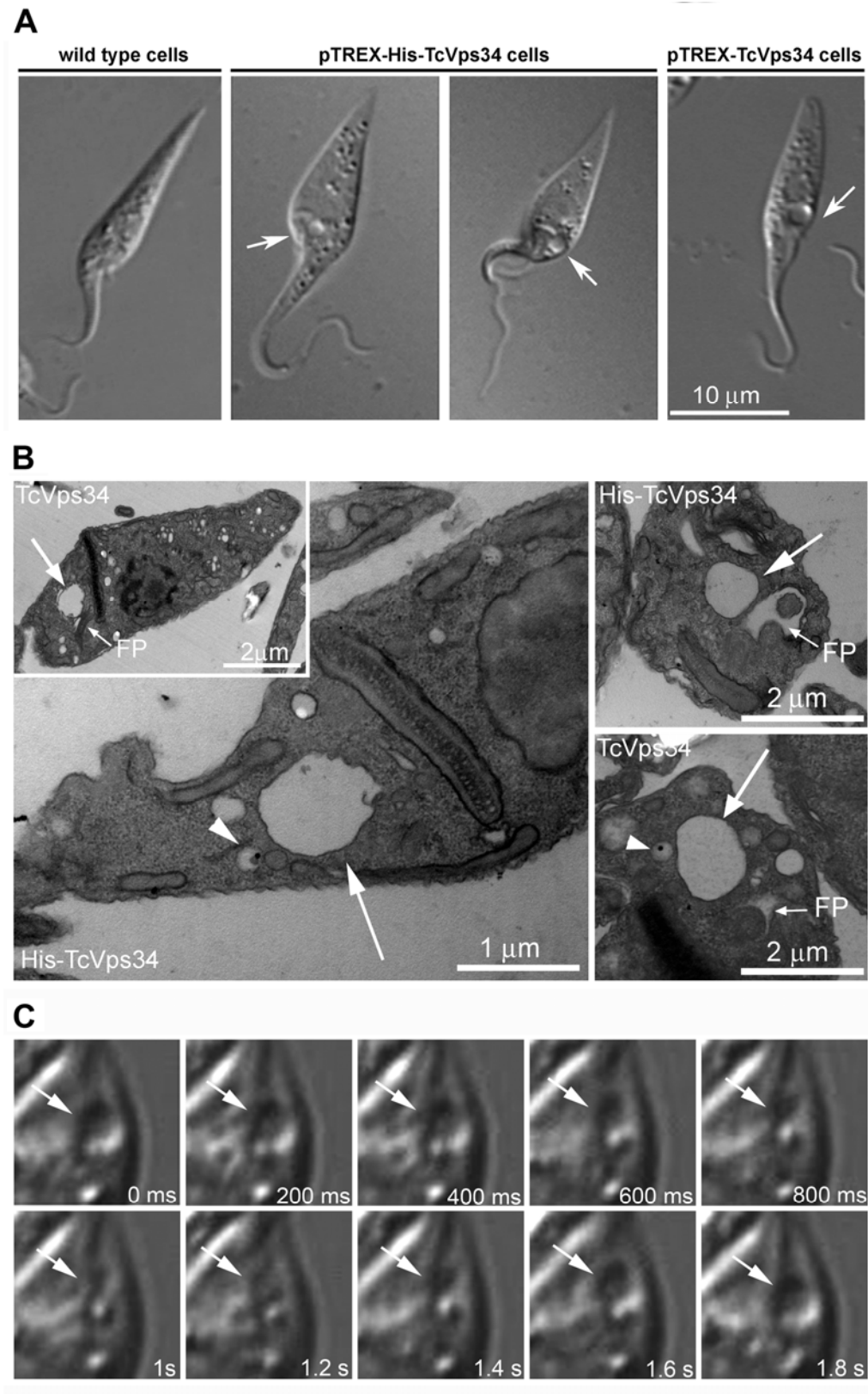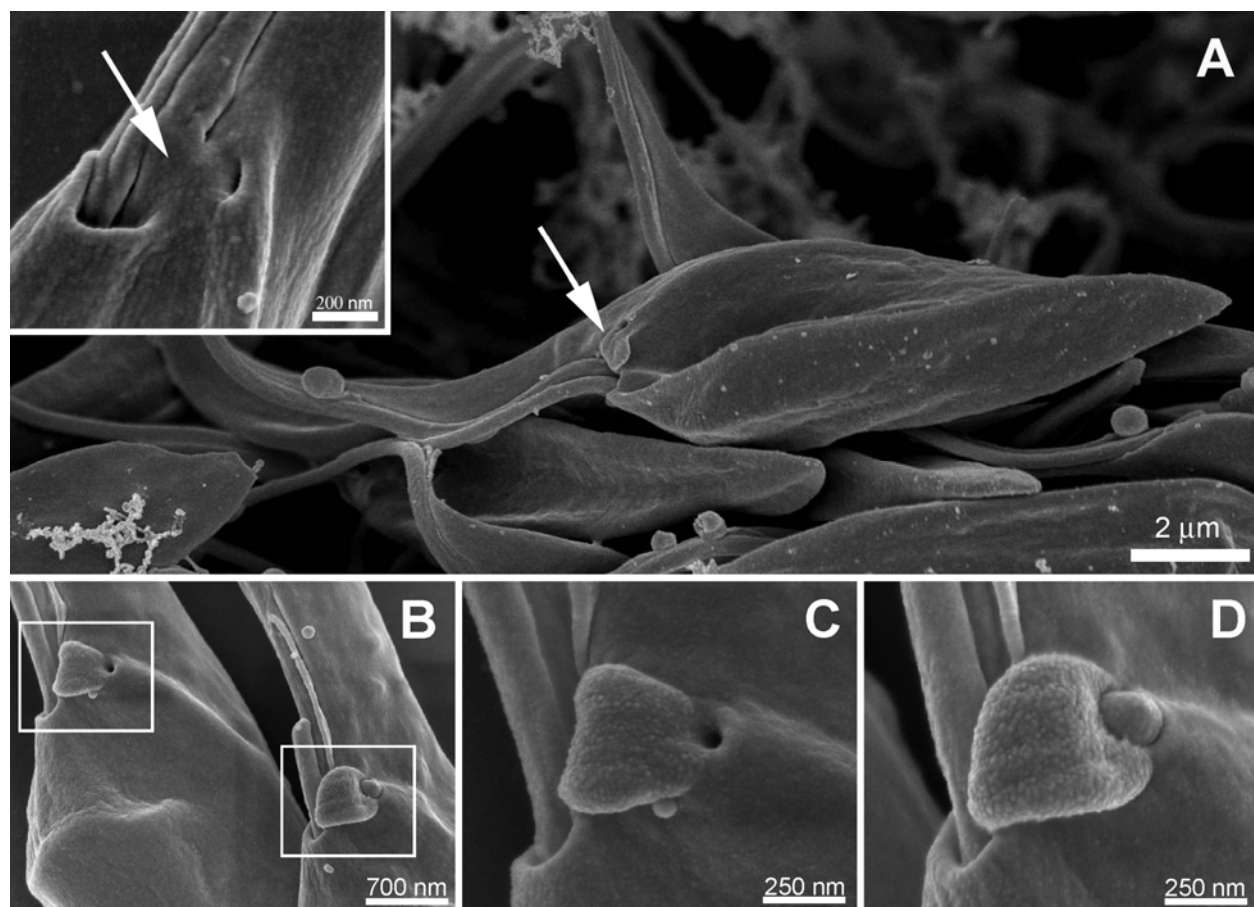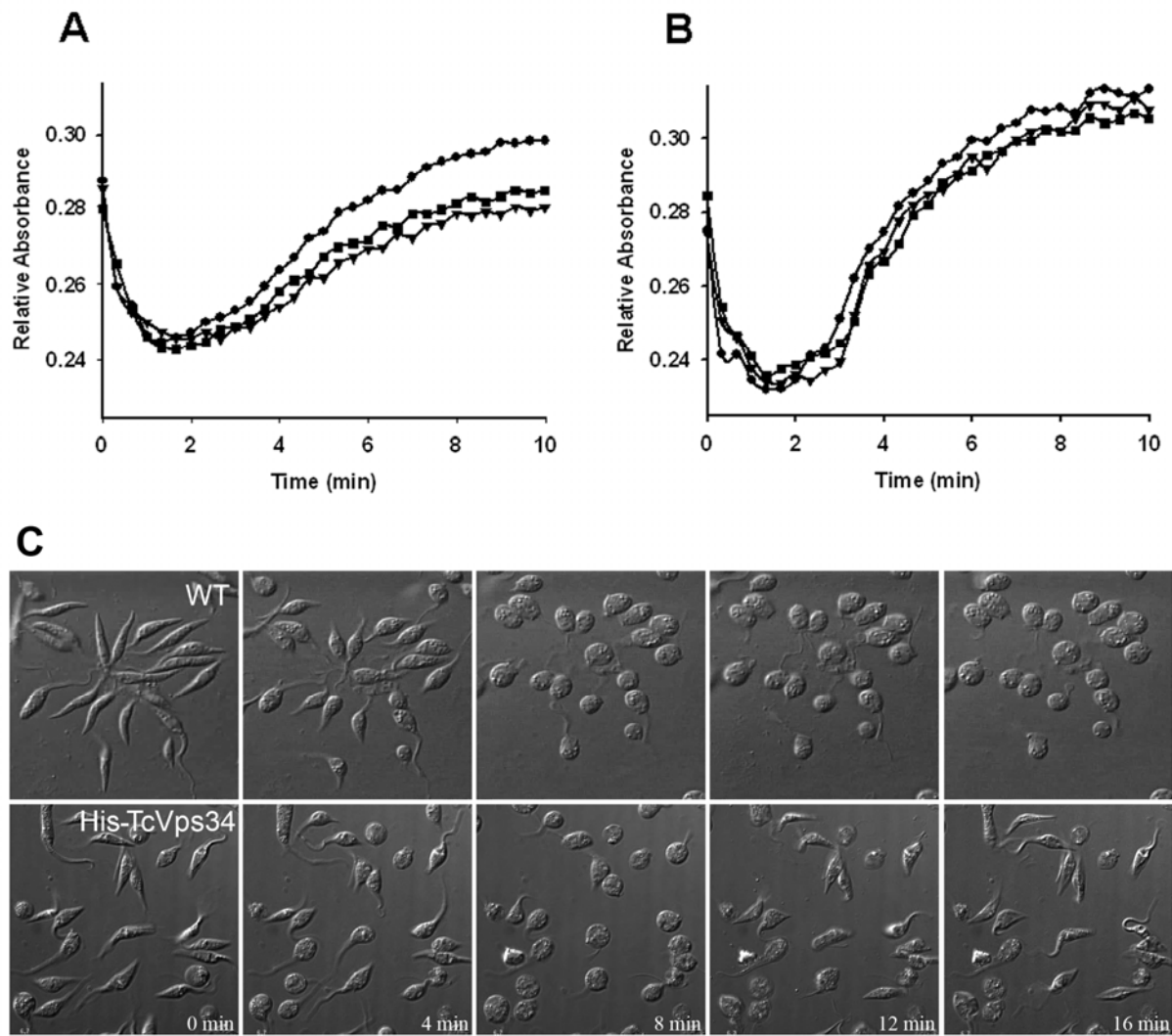
Figure 8

Figure 9

A trypanosoma cruzi phosphatidylinositol 3-kinase (TcVps34) is involved in osmoregulation and receptor-mediated endocytosis

Alejandra C. Schoijet, Kildare Miranda, Wendell Girard-Dias, Wanderley de Souza, Mirtha M. Flawiá, Héctor N. Torres, Roberto Docampo and Guillermo D. Alonso

Access the most updated version of this article at doi: 10.1074/jbc.M801367200

Alerts:
- When this article is cited
- When a correction for this article is posted

Click here to choose from all of JBC's e-mail alerts

Supplemental material:
http://www.jbc.org/content/suppl/2008/09/18/M801367200.DC1